Cohen, A. E., M. L. VanDenHeuvel, G. W. Carbin, and D. Bernhardt, 2014: The 5 June 2012 central Montana tornado event. *J. Operational Meteor.*, **2** (2), 13–26, doi: http://dx.doi.org/10.15191/nwajom.2014.0202.

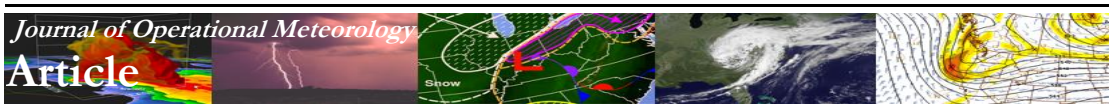

The 5 June 2012 Central Montana Tornado Event

ARIEL E. COHEN
NOAA/National Weather Service/Storm Prediction Center, Norman, Oklahoma

MEGAN L. VANDENHEUVEL
NOAA/National Weather Service, Great Falls, Montana

GREGORY W. CARBIN
NOAA/National Weather Service/Storm Prediction Center, Norman, Oklahoma

DAVID BERNHARDT
NOAA/National Weather Service, Great Falls, Montana

(Manuscript received 30 August 2013; review completed 29 January 2014)

ABSTRACT

During the afternoon and evening of 5 June 2012, central Montana experienced a rare tornado event for that region, with three confirmed tornadoes from two supercell thunderstorms. While the background environment supporting this event was generally consistent with that corresponding to a severe thunderstorm and tornado event in the midlatitudes, particular factors supporting this event in central Montana were seasonally anomalous. In support of future pattern recognition and forecasting of such an event—for which large potential impact could exist—the synoptic and mesoscale environment evolution, and the radar evolution associated with this event, are investigated. We present climatological anomalies, with midlevel lapse rates and deep moisture content being particularly high for this case. Impact-based decision support services and detailed tornado assessments from the National Weather Service in Great Falls also will be discussed.

1. Introduction

During the late afternoon and evening of 5 June 2012, central Montana experienced a rare tornado event. The combination of a strong midlevel ridge over the northern plains, an enhanced surface lee trough over the northern Rockies, ample deep moisture, high convective available potential energy (CAPE), and strong low-level and deep-layer shear over central Montana was associated with an environment that supported supercell thunderstorms.

While several severe thunderstorms occurred within the Great Falls county warning area (CWA), two distinct supercells were found to be responsible for three tornadoes affecting Meagher, Judith Basin, and Chouteau Counties (Table 1) by National Weather Service (NWS) Great Falls survey teams. On average, only one tornado occurs per 26 000 km^2 (10 000 mi^2) in Montana each year, as determined between 1991 and 2010 (Carbin 2013). Thus, three separate tornadoes emanating from multiple supercells occurring in central Montana is a rarity, as is the occurrence of long-lived supercells. No injuries or fatalities were reported as a result of these storms.

Several aspects of this event are analyzed, including climatological anomalies, the synoptic and mesoscale environment, and radar evolution. Additionally, impact-based decision support services from NWS Great Falls before, during, and after the tornado event will be discussed.

Table 1. Ratings, path lengths, and widths of the White Sulphur Springs, rural Hobson/Moccasin, and rural Big Sandy tornadoes. Length and width values are approximations.

	White Sulphur Springs Tornado	Rural Hobson/Moccasin Tornado	Rural Big Sandy Tornado
County name	Meagher	Judith Basin	Chouteau
Rating	EF1	EF0	EF0
Path length (km)	3.2	4.8	1.6
Mean width (km)	0.27	0.36	0.07

Corresponding author address: Ariel E. Cohen, NOAA/NWS/Storm Prediction Center, 120 David L. Boren Blvd., Norman, OK, 73072
E-mail: Ariel.Cohen@noaa.gov

2. Climatology

To assess climatological departures for this event, National Center for Environmental Prediction North American Regional Reanalysis data (NARR; Mesinger et al. 2006) were used to generate daily mean fields for 5 June 2012 and their departures from daily long-term means. Specifically, anomalies were determined by subtracting the 1979–2001 daily average values centered on 5 June from corresponding daily mean values on 5 June 2012 (Fig. 1). Meteorological fields that were considered include the 500-hPa geopotential height, surface–400-hPa precipitable water (PWAT), 700–500-hPa lapse rate, and 850–500-hPa shear vector magnitude. These images (Fig. 1) illustrate the highly anomalous patterns in the parameters for this event, especially for midlevel lapse rate and shear, which played a significant role in supporting organized, intense convection.

To further contextualize the climatological rareness of this event, similar large-scale patterns were identified between the 5 June 2012 event and other days from the NARR dataset (1979–2009). In particular, patterns of 500- and 850-hPa geopotential height and PWAT that quantitatively best matched those from 5 June 2012 were systematically selected. By determining root mean square errors (RMSEs) between matching pairs, top analogs for the 5 June 2012 event were identified and listed in order of increasing RMSE (Table 2). This process of determining best-matching analogs provides a systematic approach to quantitatively selecting similar patterns whose associations with sensible weather (e.g., severe convection) may be ascertained. Differences between these similar patterns

Table 2. Top analog dates (relative to 5 June 2012) for 500- and 850-hPa heights and PWAT from the NARR dataset listed in order of increasing RMSE.

Top 4 analog dates of 500-hPa heights	Top 4 analog dates of 850-hPa heights	Top 4 analog dates of PWAT
5 June 1997	5 June 1997	22 May 2008
25 May 1990	19 April 2007	24 May 2006
16 May 1984	21 April 1997	2 June 2005
24 May 1990	18 March 2001	6 June 1988

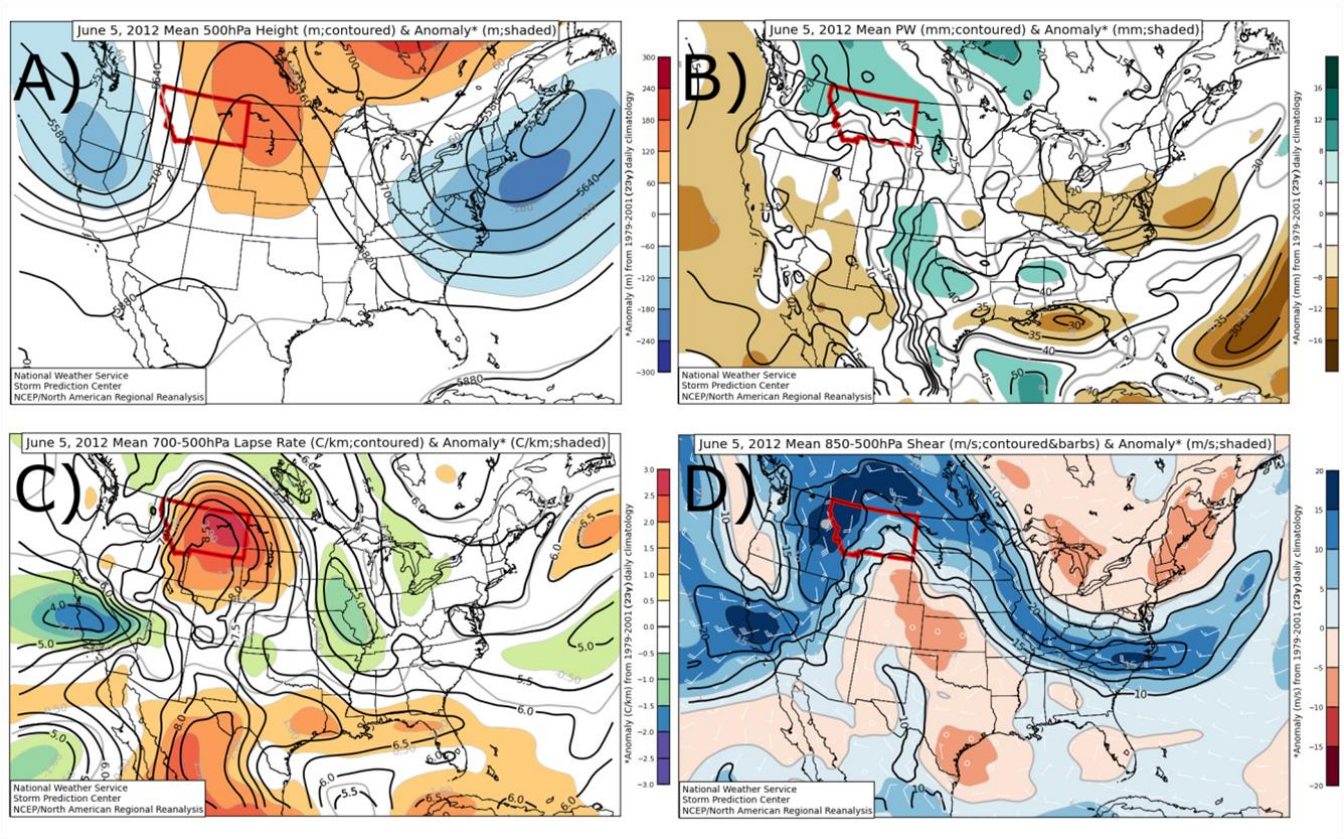

Figure 1. The 5 June 2012 mean a) 500-hPa height (m), b) PWAT (mm), c) 700–500-hPa lapse rates (°C km^{-1}), and d) 850–500-hPa shear vector magnitude (m s^{-1}). Departures from the 1979–2001 daily mean centered on 5 June are shaded with the legend to the right of each panel. Montana is outlined with a thick red line. *Click image for an external version; this applies to all figures hereafter.*

and corresponding NARR data on 5 June 2012 are presented in Fig. 2.

Note that the NARR data used for the generation of Fig. 1 cover a longer time span compared to Fig. 2. This is the result of using two separate subsets of available NARR data that exhibit variations in temporal frequency. In particular, Fig. 1 uses daily meteorological values in the computations of anomalies over a relatively shorter time period than Fig. 2, which uses individual times throughout the day for the purposes of analog retrieval over a longer time period. The systematically smaller-scale spatiotemporal pattern matching invoked in analog retrieval deems it necessary to use the individual times for determining analog matches, and thus the longer-period dataset for Fig. 2. On the other hand, the shorter-period dataset that combines individual times would be more appropriate to specify anomalies based on larger spatiotemporal scales, which are the foci of Fig. 1.

In the case of the best matches to 5 June 2012, the 500-hPa anomalies (Fig. 2a) suggest that troughs of similar strength have occurred near Montana on past days in May and June. It is the strength and amplitude of the 500-hPa downstream ridge that distinguishes 5 June 2012 from the corresponding best matches. The 850-hPa anomalies reveal the 5 June 2012 event to have a stronger low-level cyclone near the border of Montana/Wyoming (Fig. 2b) than on previous analog days. Three of the four best-matching analog dates for 850 hPa also correspond to cooler season patterns in March and April when the strength of the low-level flow typically is greater. Last, the PWAT on 5 June 2012, when compared to best-matching analogs, was characterized by a discontinuous plume of greater tropospheric moisture from the Great Plains northwestward to the northern Rockies (Fig. 2c). Tornado reports that correspond to the best-matching analogs (Table 2) for 5 June 2012 are shown in Fig. 3. This image suggests that past patterns most similar to that of 5 June 2012 are indeed conducive to severe weather in this part of the country. Presumably, smaller differences between patterns for 5 June 2012 and its corresponding best-matching analogs imply that the analog pattern is a close fit to 5 June. In turn, this could lend credence to the notion that the ensuing sensible weather (e.g., severe weather) for the best-

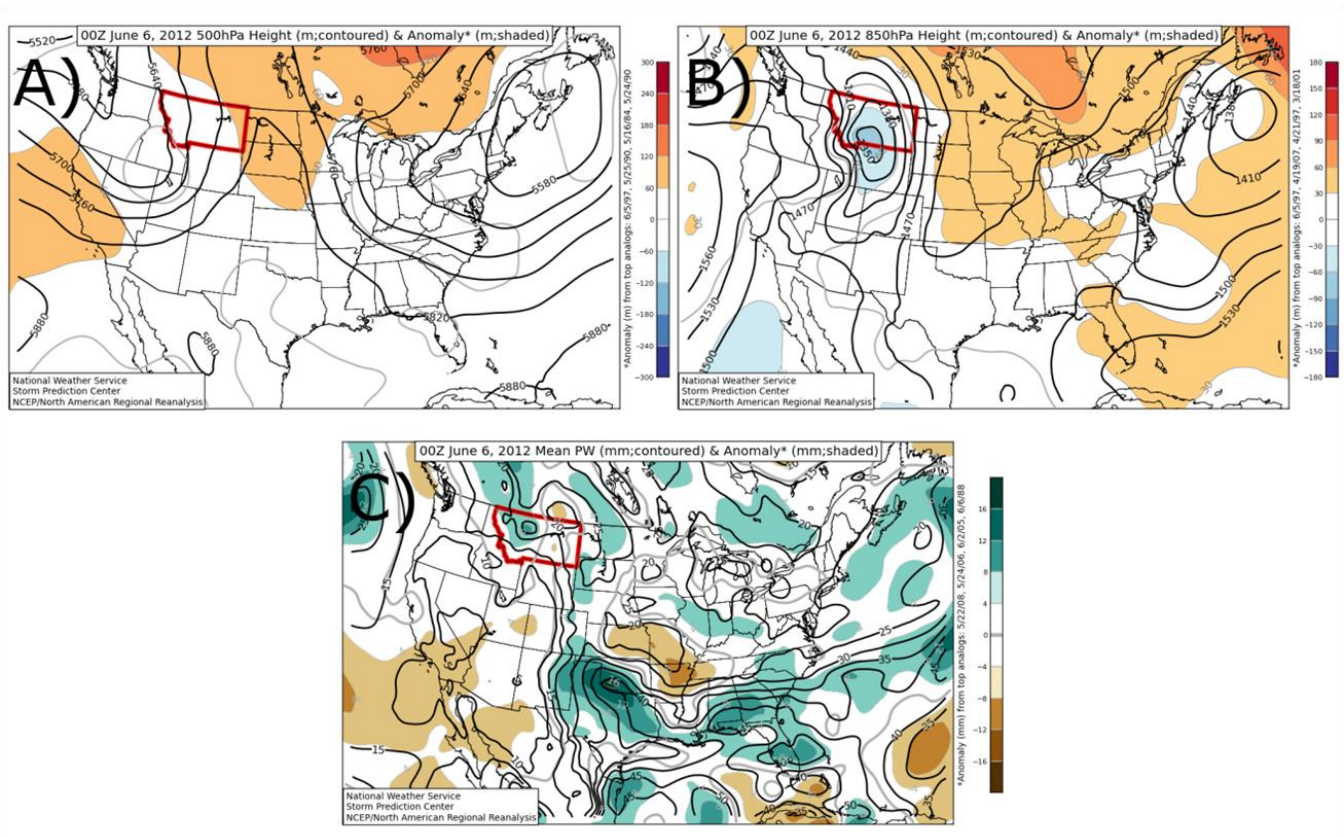

Figure 2. The 0000 UTC 6 June 2012 a) 500-hPa height (m), b) 850-hPa height (m), and c) PWAT (mm), along with the departure (shaded) from the top four analogs. The analog dates are indicated next to the color bar on the right of the graphic, and also given in Table 2.

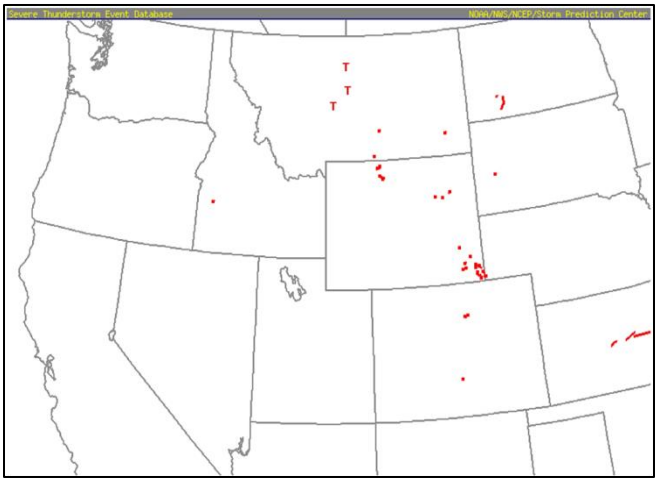

Figure 3. All tornado events (red dots/paths) from (i) the best analogs in Table 2 and (ii) 5 June 2012 (red "Ts"). Six of the eleven unique best analog dates in Table 2 correspond with tornado days; these include 6 June 1988, 24 May 1990, 25 May 1990, 21 April 1997, 5 June 1997, and 2 June 2005.

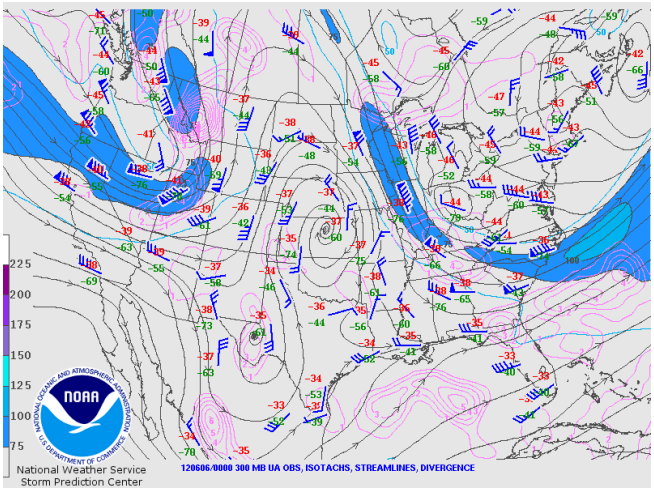

Figure 4. 300-hPa observations and objectively analyzed streamlines (gray), divergence (pink, 1×10^{-5} s^{-1}), and isotachs [color fill >75 kt (38 m s^{-1}) per legend at left] for 0000 UTC 6 June 2012.

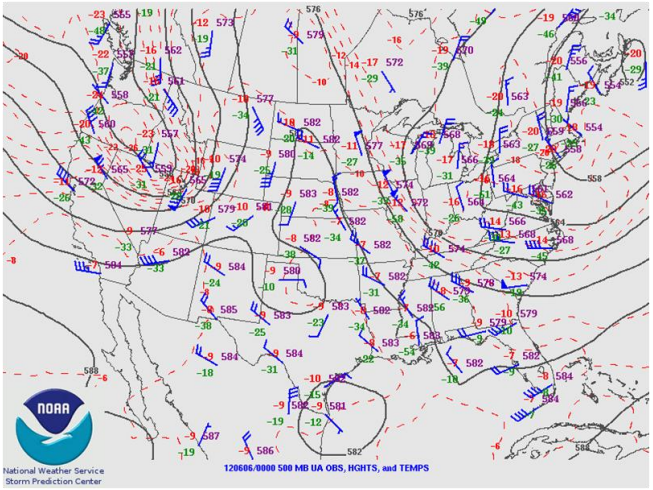

Figure 5. 500-hPa observations and objectively analyzed heights (dam, gray) and isotherms (°C, dashed red) for 0000 UTC 6 June 2012.

matching analogs could be in the realm of possibility for the corresponding forecast period.

3. Synoptic and mesoscale setup

This section addresses the background meteorological environment via an ingredients-based approach, highlighting aspects of moisture, lift, instability, and vertical wind shear that aligned to support the severe weather episode. These characteristics are largely associated with the climatologically deviating patterns described above.

a. Relevant features above the surface

The evening of 5 June 2012 featured a well-defined, negatively tilted short-wave trough extending from the Pacific Northwest southeastward into the Great Basin (Fig. 4). Strong upper-level divergence was found to coexist with a region of diffluence atop an inferred region of strong, deep ascent overlaying western Montana between the short-wave trough axis and a downstream ridge axis over the central and northern plains. The negative tilt of the short-wave trough was accompanied by southeasterly to southerly flow in the upper levels (Fig. 4) and midlevels (Fig. 5), with speeds around 18 m s^{-1} (35 kt) at 500-hPa (Fig. 5), contributing to strong vertical wind shear through a deep layer of the lower-to-middle troposphere.

The short-wave trough was accompanied by a strong front that tilted westward from 850 hPa (Fig. 6) to 700 hPa (Fig. 7) to 500 hPa (Fig. 5). And, with a corresponding intense cyclone noted at the 850- and 700-hPa levels (Figs. 6 and 7, respectively), strong 850- to 700-hPa southeast winds were noted over the high plains of Montana, with winds exhibiting slight veering with increasing height between these levels. This southeasterly current was accompanied by both strong vertical wind shear in the lower levels as noted on the Glasgow, Montana, soundings (e.g., Fig. 8), as well as an influx of moisture likely originating from the Gulf of Mexico before traversing the Great Plains.

b. Features at the surface

A subjectively analyzed surface chart at 2000 UTC 5 June 2012 (i.e., around the time of convective

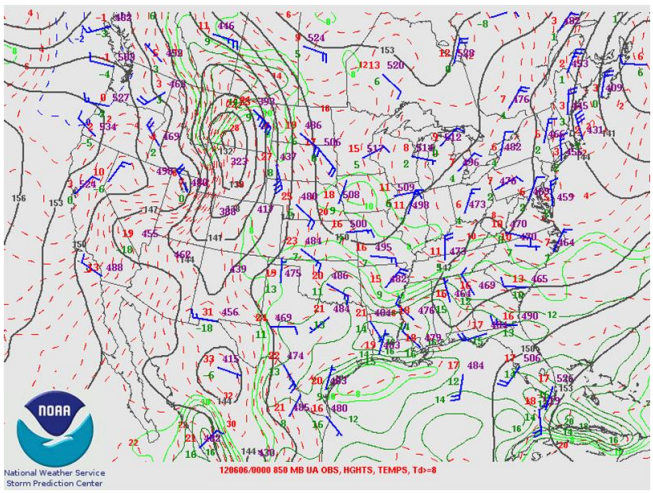

Figure 6. 850-hPa observations and objectively analyzed heights (gray, dam), isotherms (°C, dashed red), and isodrosotherms (°C, green) at 0000 UTC 6 June 2012.

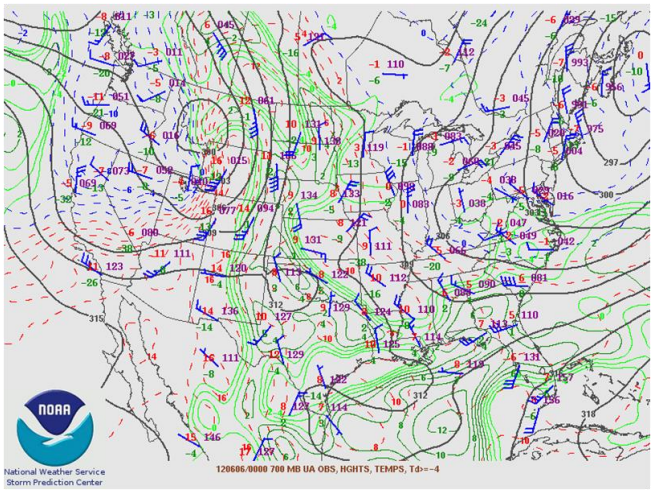

Figure 7. Same as Fig. 6 but for 700-hPa.

initiation over the mountains of south-central Montana, Fig. 10) further highlights the supportive environment of this severe weather episode over Montana. Rich low-level moisture, featuring surface dewpoints from 14 to 17°C (57 to 63°F), was common north of a warm front lying east of a surface low between Bozeman and Livingston, Montana. These are associated with anomalously high PWAT values as established in Fig. 1 and Fig. 2.

South-southeasterly flow at the surface advected hot air into eastern Montana, resulting in a north-northwestward surge in the warm front with temperatures south of the front reaching 34–37°C (94–99°F) across east-central and southeastern Montana. While relatively stronger vertical mixing south of the front allowed dewpoints to fall to 4–9°C (40–49°F), higher

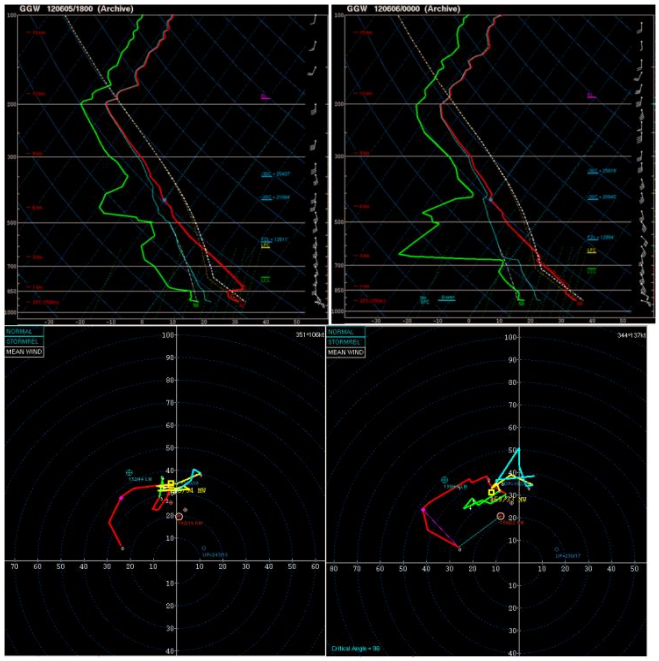

Figure 8. Observed soundings at 1800 UTC 5 June 2012 (left) and 0000 UTC 6 June 2012 (right) at Glasgow, MT. Red lines depict environmental temperature, green lines depict environmental dewpoints, and dashed white lines depict parcel temperature traces for the surface-based parcel. Corresponding hodographs are plotted below the individual soundings. Small white numbers beside the hodographs indicate height above ground level (AGL, km).

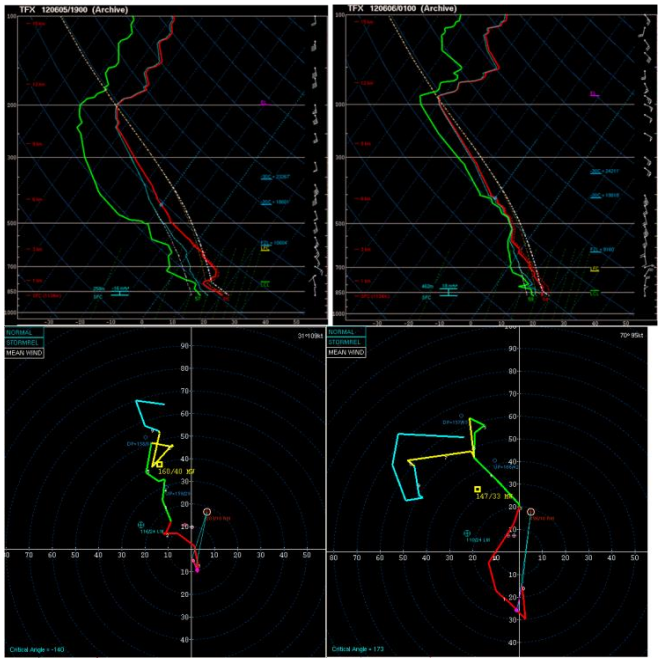

Figure 9. Same as Fig. 8 except for 1900 UTC 5 June 2012 (left) and 0100 UTC 6 June 2012 (right) at Great Falls, MT.

dewpoints were found farther north toward the moist axes, where modestly lower surface temperatures were

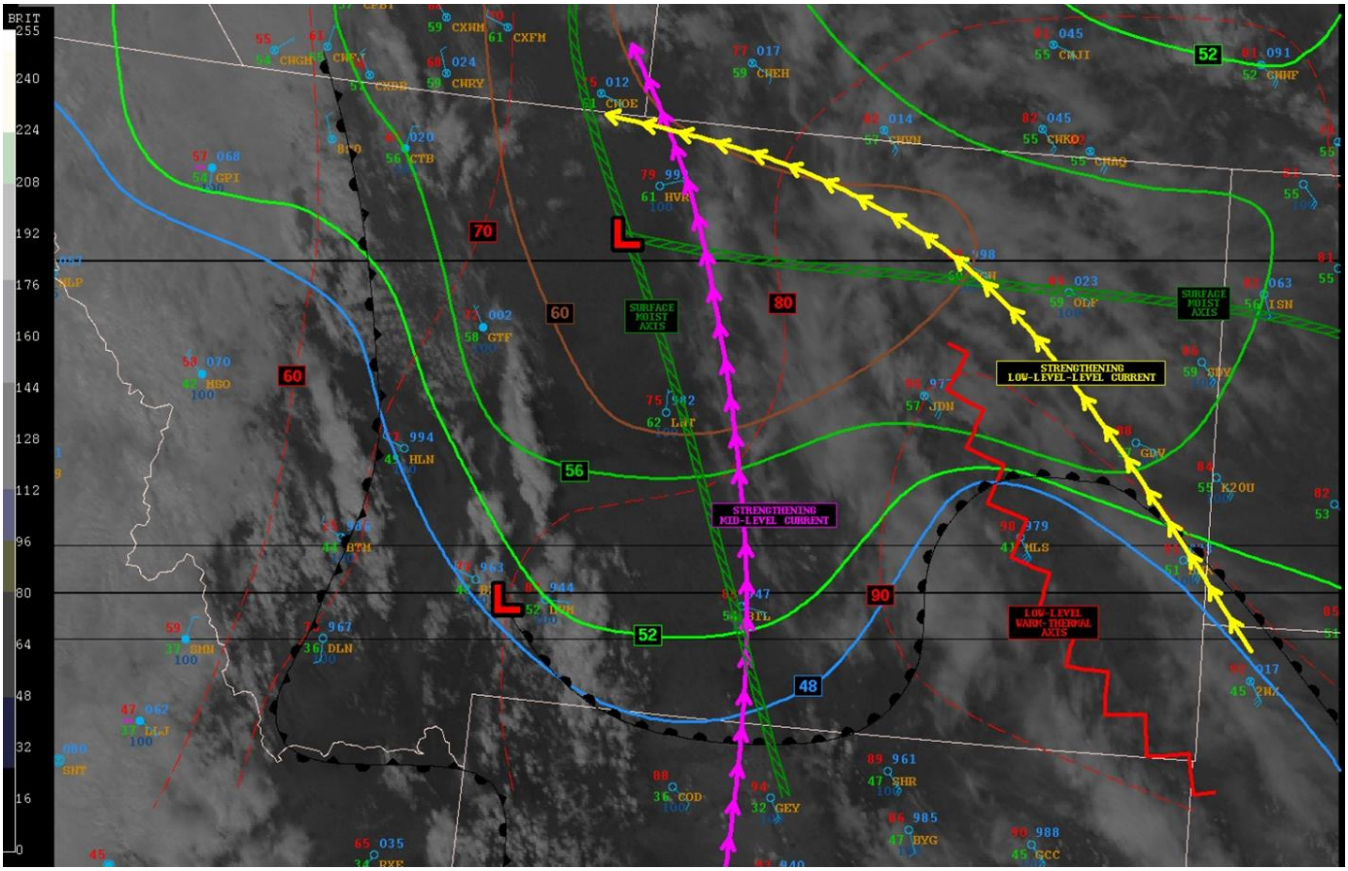

Figure 10. Visible satellite image from the *Geostationary Operational Environmental Satellite-13 (GOES-13)* at 2002 UTC 5 June 2012. Overlaid are the 2000 UTC 5 June 2012 Meteorological Aerodrome Reports (METARs), as well as a manually analyzed surface chart including isotherms [dashed red contours every 5.6°C (10°F)], isodrosotherms [solid blue, green, and brown contours every 2.2°C (4°F)], a low-pressure center (red letter "L"), and depictions of salient features near the surface and aloft. Surface fronts are in black as opposed to conventional colors in order to distinguish them from other colored features and contours.

present. The region of drier, warmer air extended west-southwestward across northern Wyoming, generally south of the warm front. Thus, this warm front, to some extent, resembled a dryline, north of which rich low-level moisture was present. Lift—emanating from the circulation accompanying the warm front—likely augmented orographic circulations close to the surface low, located near Bozeman. This is where convection initiation was noted per cumulus build-ups on visible satellite imagery.

Overlaying representations of salient currents aloft on top of the surface chart (e.g., Fig. 10) suggests a wind profile that veered with increasing height, and the corresponding vertical shear increased in response to the approaching short-wave trough. As indicated already, routine and special soundings were taken at Glasgow and Great Falls, Montana, before and during the event. These soundings, including corresponding hodographs, are displayed in Figs. 8 and 9.

The wind profiles and hodographs represent notable changes in wind speed and direction with increasing height through the troposphere, highlighting the strong deep-layer wind shear in place with vertically veering flow through a deep layer. Storm-relative helicity within the 0–1-km and 0–3-km layers ranged from 200 to 300 $m^2\ s^{-2}$ at Glasgow (Fig. 8), with slightly lower values observed in the Great Falls soundings (e.g., Fig. 9). However, at both locations, an increase in helicity through time was noted in tandem with an elongation of the hodograph, likely in response to the approaching short-wave trough. Low-level directional shear was enhanced at Great Falls by the northerly wind component near and just above the ground. Such values of helicity amidst 1500–2000 J kg^{-1} of mean-layer CAPE and 18 m s^{-1} (35 kt) to 26 m s^{-1} (50 kt) of effective bulk shear vector magnitude (approximated from model objective analysis output) would provide concern for the threat of tornadic

supercells (e.g., Thompson et al. 2003). This degree of buoyancy was aided by steep midlevel lapse rates of 8–9°C km^{-1}, though the influence of convection at Great Falls provided a slight reduction of 700–500-hPa lapse rates at 0000 UTC. Consistent with this expectation, the majority of high-resolution numerical weather prediction model guidance generated during the day leading up to this event exhibited robust convective structures—including supercells and intense line segments.

4. Outlook/watch/warning services overview, radar evolution, and local terrain effects

Prior to the initiation of severe thunderstorms, a coordination call between NWS Great Falls and the Storm Prediction Center (SPC) in Norman, Oklahoma, prompted a tornado watch effective from 2030 UTC 5 June until 0500 UTC 6 June for much of central and north-central Montana. A severe thunderstorm watch also was in effect until 0300 UTC 6 June for parts of southwestern Montana. Thunderstorms developed shortly after the tornado watch was issued. Figure 11 illustrates some of the graphical products issued by the SPC leading up to the event.

Base and derived Weather Surveillance Radar-1988 Doppler (WSR-88D) level II data were studied using the GR2Analyst software (www.grlevelx.com/gr2analyst/) to investigate storm-scale evolution for the 5 June 2012 tornado event. A radar animation is provided in Fig. 12. Two distinct supercells will be assessed and will be referenced in graphs and tables that follow. "Supercell 1" references the storm that produced a tornado in White Sulphur Springs and "supercell 2" references the storm that produced a tornado near Hobson and Big Sandy. See Fig. 13 for a map with highlighted geographical references.

a. Supercell 1

Time series of the 0.5-degree average rotational velocity and maximum gate-to-gate shear based on storm-relative motion (SRM) for supercell 1 are provided in Figs. 14 and 15, respectively. In the present work, "average rotational velocity" refers to the arithmetic mean of the absolute value of the maximum inbound velocity and the absolute value of the maximum outbound velocity accompanying the larger mesocyclone. "Maximum gate-to-gate shear" refers to the sum of the absolute values of immediately

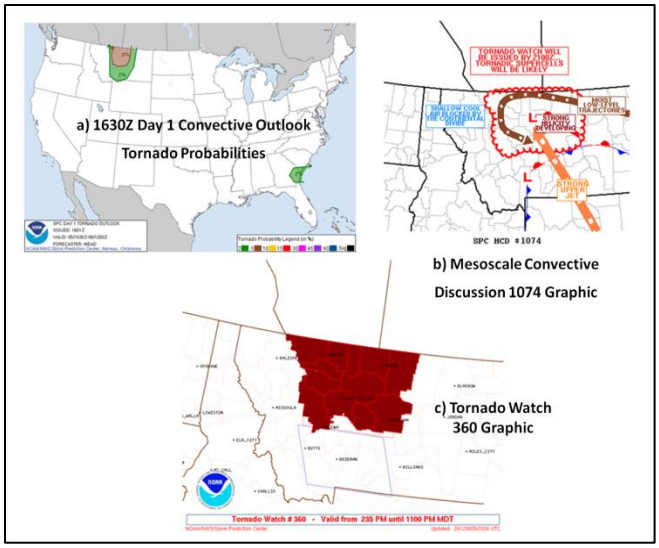

Figure 11. SPC products for a) 1630 UTC 5 June 2012 convective outlook tornado probabilities, b) mesoscale discussion graphic prior to issuance of tornado watch, and c) tornado watch (in red color fill) and outline of severe thunderstorm watch (in light blue).

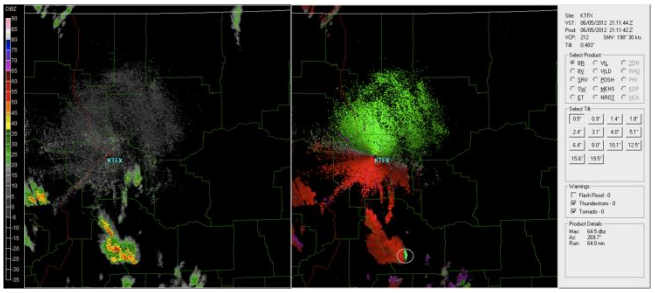

Figure 12. Radar reflectivity (left) and SRM (right) at 0.5 degrees from the KTFX WSR-88D valid 2112 UTC 5 June 2012. Ellipses are placed in the right panel to highlight the approximate location of any identifiable mesocyclone (nontornadic in white and tornadic in yellow per NWS Great Falls survey information). *Click image for an external animation valid 2112–0315 UTC 5–6 June 2012.*

Figure 13. Map of highlighted geographical references discussed throughout the paper.

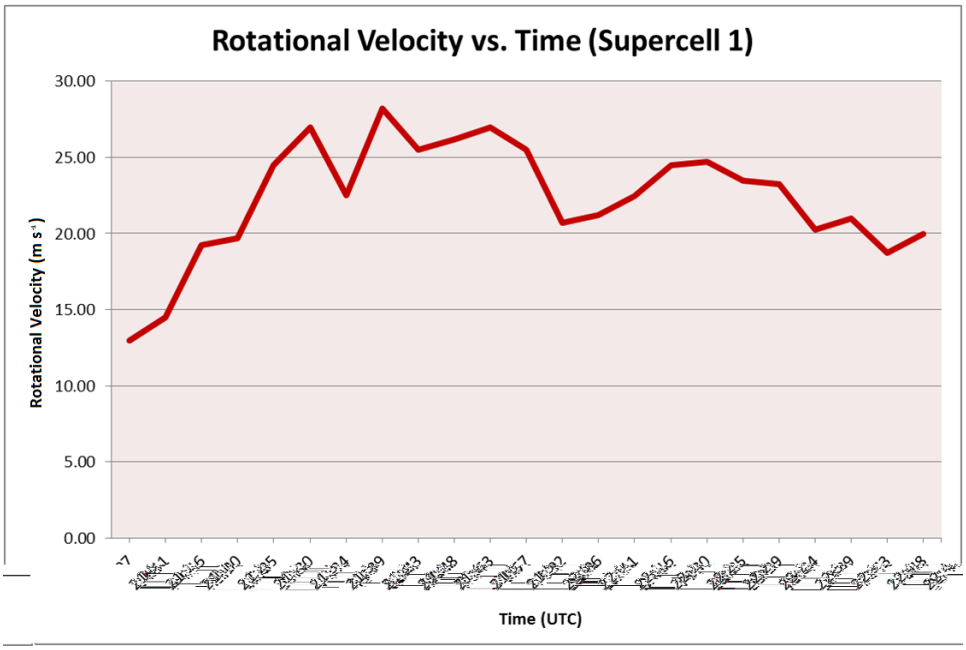

Figure 14. Time series of average rotational velocity (m s^{-1}) for the duration of the first tornadic supercell on 5 June 2012 that produced a tornado in White Sulphur Springs.

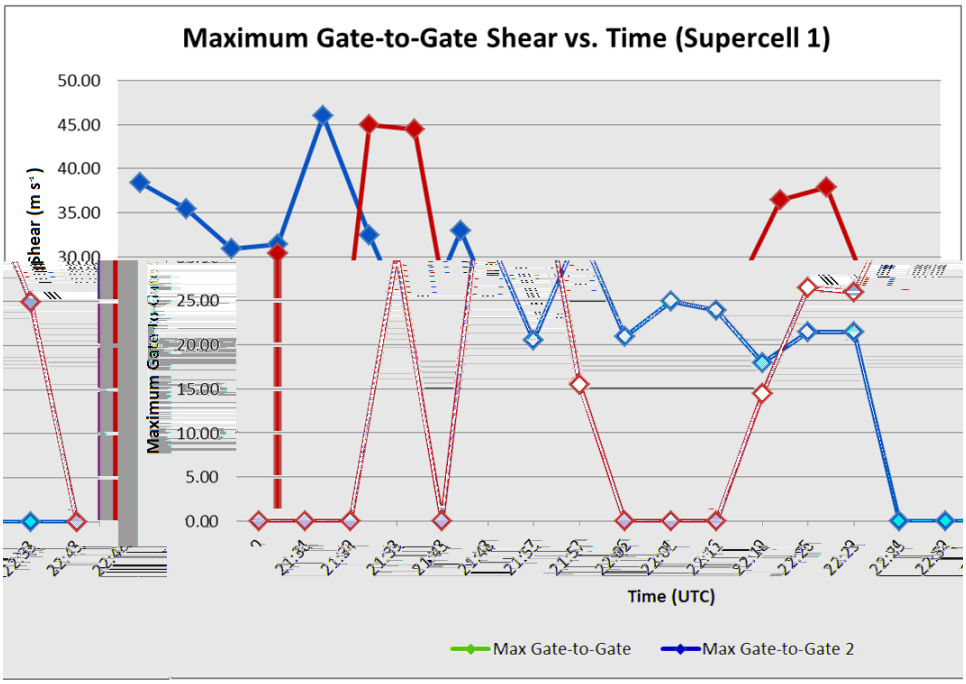

Figure 15. Times series of maximum gate-to-gate shear (m s^{-1}) for the duration of the first tornadic supercell on 5 June 2012 that produced a tornado in White Sulphur Springs. It is unclear if the two separate time series represented different tornadoes, thus two individual maximum gate-to-gate shear values associated with separate, intense, tight rotational couplets embedded within the larger supercell are provided.

adjacent inbound and outbound velocities at constant range from the radar following the motion (i.e., a Lagrangian framework) of the most intense, persistent, tight circulation (i.e., the maximum sum of absolute values) emanating from adjacent radar gates yielding rotation—as opposed to divergence. Thus, the term "maximum" refers to traceable relative maxima in the most intense rotational couplets. Figure 15 reflects the

evolution of two separate, intense, tight rotational couplets embedded within the larger supercell. Time series of maximum gate-to-gate shear values are provided for individual identifiable rotational couplets, with each time series indicating a separate, generally persistent, couplet.

Around 2000 UTC, supercell 1 developed in northern Gallatin County near the Bridger Mountains. For the next hour, the strength of the storm fluctuated, but showed signs of increased intensity with an organized midlevel circulation as it moved near the Bridger Mountains. Shortly before 2100 UTC, this storm began to split, and the dominant cell turned right as a weak echo region (WER) formed. At 2105 UTC, NWS Great Falls issued a severe thunderstorm warning. By 2106 UTC, the 0.5-degree SRM data indicated an inflow notch and a mesoscale circulation with a rotational velocity of 19 m s^{-1} (37 kt).

As the cell exited areas of complex terrain, it took a northward track toward White Sulphur Springs, which is located south of the Little Belt Mountains in central Meagher County (Fig. 13). By 2130 UTC, the cell continued to indicate supercell characteristics with a strong mesocyclone, increased rotational velocity of 27 m s^{-1} (53 kt), and a rotational couplet with gate-to-gate shear of 39 m s^{-1} (75 kt) at the 0.5-degree tilt. Despite these strong mesocyclone signatures, the storm was over 110 km from the Great Falls (KTFX) radar, and may not be an accurate representation of the lower-level storm characteristics.

A new severe thunderstorm warning was issued for Meagher County at 2138 UTC. The warning mentioned (i) Doppler radar-indicated weak rotation within the storm and (ii) while not immediately likely, a tornado could develop. At 2140 UTC, NWS Great Falls received the first public report of funnel clouds near White Sulphur Springs. Reports of ping-pong and golf-ball sized hail also were relayed. A tornado warning was issued for central Meagher County including White Sulphur Springs at 2149 UTC. Around the time of warning issuance, a bounded WER (BWER) was present, rotational velocity was estimated at 26 m s^{-1} (51 kt), and a rotational couplet contained gate-to-gate shear of 46 m s^{-1} (89 kt). This gate-to-gate shear value was the highest value recorded for this particular storm.

Subsequent scans showed the storm continuing to turn right; gate-to-gate shear for the aforementioned couplet decreased to 33 m s^{-1} (64 kt) and rotational velocity decreased to 21 m s^{-1} (40 kt) by 2202 UTC. As the cell began to move over higher terrain in the Little Belt Mountains, it continued to have a well-defined mesocyclone structure; however, the cell was more disorganized, and a BWER was no longer present. As the cell continued to move over the Little Belt Mountains, the storm weakened further with no additional reports of severe weather.

b. Supercell 2

While the supercell thunderstorm in Meagher County was weakening, another supercell was developing and strengthening outside of the NWS Great Falls CWA in Wheatland County (NWS Billings CWA). This storm (supercell 2) moved into Judith Basin County in the NWS Great Falls CWA around 2310 UTC. Time series of the 0.5-degree average rotational velocity and maximum gate-to-gate shear based on 0.5-degree SRM for supercell 2 are provided in Figs. 16 and 17, respectively. Calculations of these quantities follow identical procedures as those followed in the generation of Figs. 14 and 15, as discussed in the preceding subsection.

With supercell 2 exhibiting several rotational signatures and a strong inflow notch [outbound velocities >36 m s^{-1} (70 kt)], a severe thunderstorm warning was issued at 2313 UTC for parts of Meagher and Judith Basin Counties. By 2324 UTC as this storm continued organizing, it developed a BWER. While a couplet containing gate-to-gate shear at 45 m s^{-1} (87 kt) was noted, this signature was over 110 km from the KTFX radar at an elevation of approximately 1.8 km AGL.

Rotational velocity increased from 27 m s^{-1} (53 kt) at 2324 UTC to 40 m s^{-1} (77 kt) at 2334 UTC with two separate, intense couplets noted with relatively large gate-to-gate shear values: 51 m s^{-1} (99 kt) and 56 m s^{-1} (109 kt). A three-body scatter spike (Lemon 1998) also was observed on the southeastern side of the storm. Reflectivity values were >70 dBZ up to 9.1 km AGL. A weather spotter reported golf-ball size hail 11.3 km (7 mi) south-southwest of Utica, Montana, at 2330 UTC. Radar showed that the two gate-to-gate shear maxima persisted—about 5.5 km apart at 2330 UTC.

The location of the BWER coincided with the maximum gate-to-gate shear values around 40 m s^{-1} (77 kt and 78 kt) (Fig. 17). The NWS in Great Falls issued a tornado warning at 2340 UTC for west-central Fergus County and eastern Judith Basin County effective until 0015 UTC (all times after 0000 UTC refer to 6 June 2012). A public report of a tornado with damage was received at 2341 UTC, and a 40-m s^{-1} (90 mph) wind gust was reported by an NWS cooperative weather observer in Hobson at 2348 UTC.

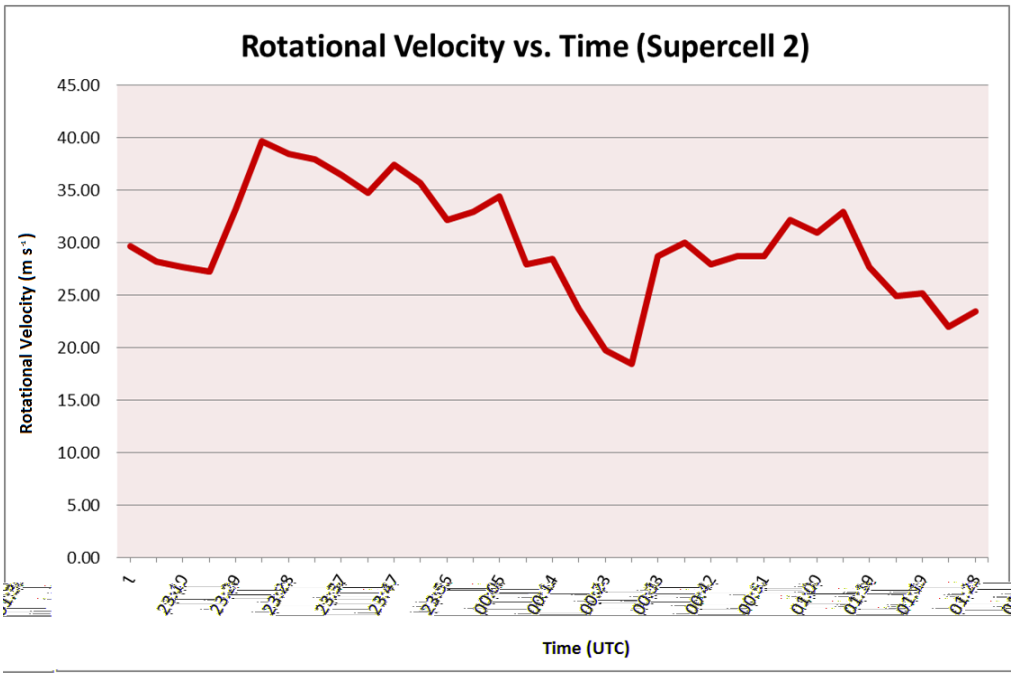

Figure 16. Same as Fig. 14 except for the second tornadic supercell on 5–6 June 2012 (UTC) that produced a tornado near Hobson and Big Sandy.

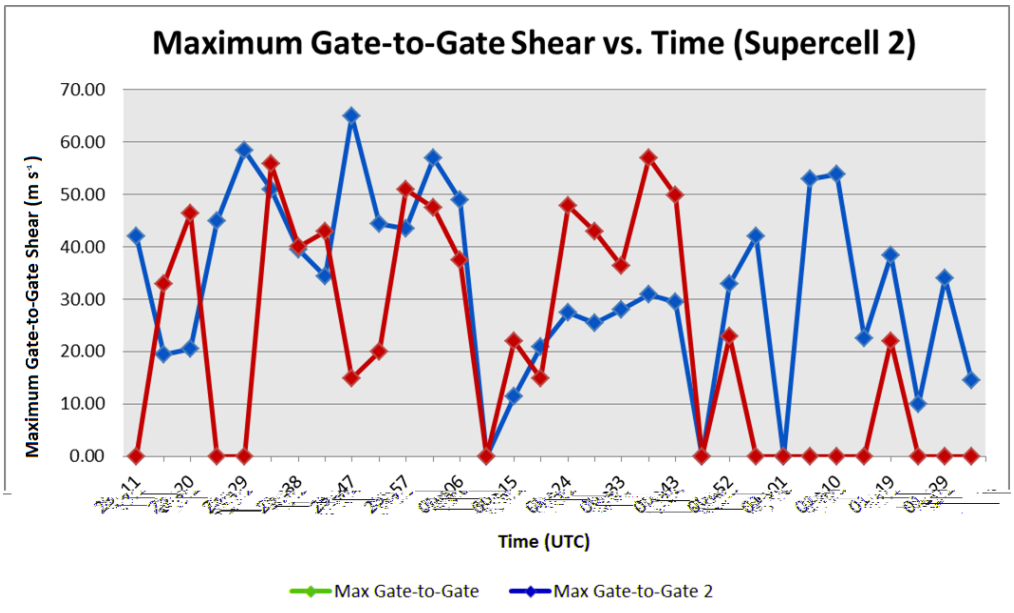

Figure 17. Same as Fig. 15 except for the second tornadic supercell on 5–6 June 2012 that produced a tornado near Hobson and Big Sandy.

This supercell continued to show tight, strong circulations embedded within the broader strong mesocyclone with, at least two gate-to-gate shear maxima through 0006 UTC and an average rotational velocity of 36 m s^{-1} (70 kt). The supercell crossed State Highway 200 approximately 4 km east of Moccasin in Judith Basin County. Quarter-size hail and a rotating wall cloud were reported by a trained spotter approximately 11 km (7 mi) northwest of Moccasin at 2350 UTC. Because the storm remained at least 110 km from the radar at an elevation of approximately 1.8 km (5.8 kft) AGL, low-level

features of the storm were difficult to distinguish. A photo taken by storm chasers showed a tornado, which prompted a new tornado warning to be issued for west-central Fergus County, east-central Judith Basin County, and extreme south-central Chouteau County at 0011 UTC—effective through 0100 UTC. Shortly after the new tornado warning was issued, reports of ping-pong sized hail and a funnel cloud were received from the Denton area near the border of Fergus and Judith Basin Counties. In addition, 45-m s^{-1} (100 mph) winds were reported in the Danvers area in Fergus County at 0012 UTC, with some damage to trees and hay bales.

Though the average maximum rotational velocity decreased to 26 m s^{-1} (50 kt) between 0015 UTC and 0043 UTC (Fig. 16), the cell maintained a broad, strong mesocyclone with two notable maximum gate-to-gate shear values (Fig. 17). Despite no official tornado reports, the supercell signatures indicated on radar imagery prompted a tornado warning for northwestern Fergus County, southwestern Blaine County, and eastern Chouteau County from 0052 UTC until 0115 UTC. The storm increased in intensity with a calculated rotational velocity of over 31 m s^{-1} (60 kt) and a couplet containing a gate-to-gate shear value of >51 m s^{-1} (100 kt) at 0106 UTC and 0110 UTC. A public report of at least quarter-sized hail was received from 26 km (16 mi) east of Geraldine at 0055 UTC, and no additional severe weather reports were received from Fergus County.

Even though these signatures were over 110 km northeast of the radar, the maintenance of storm intensity and its history of producing tornadoes prompted this issuance of a new tornado warning for northwestern Fergus County, southwestern Blaine County, and eastern Chouteau County until 0130 UTC, which extended into west-central Blaine County and northeastern Chouteau County until 0215 UTC. As the storm continued to move north-northeastward, radar signatures were becoming increasingly difficult to analyze. However, at 0133 UTC storm spotters reported and confirmed a cone tornado approximately 13 km south-southeast of Big Sandy in Chouteau County. A trained spotter also reported golf-ball sized hail at 0158 UTC. After 0158 UTC, no further tornado or severe weather reports were received. As the storm moved farther than 150 km from the KTFX radar, the rotational velocity along with any possible enhanced gate-to-gate shear signatures decreased with each subsequent volume scan, and the storm moved into Canada at 0319 UTC.

c. Local terrain effects

The terrain complexities across portions of central and north-central Montana may indeed have played a role in modulating convective trends after convection already developed (e.g., around the Little Belt Mountains). However, specific topography-related impacts on convection would be highly speculative without further investigation using a more spatiotemporally dense observing network and/or high-resolution model simulations. Such work is outside the scope of the present study, though orographic effects have been known to affect the evolution of convective processes elsewhere (e.g., Bosart et al. 2006). Regardless, convection-preceding orographic ascent appears to have been at least partly responsible for the initiation of this convection, as evidenced by the spatial alignment between initial convective towers and topographic elevated heat sources (Fig. 10). Previous work reveals conditional linkages between the existence of mountains and the development of convection (e.g., Banta and Schaaf 1987; Tucker and Crook 2001).

5. Post-storm damage assessments

Reports of a possible tornado in White Sulphur Springs occurred at 2140 UTC 5 June 2012, and a post-storm assessment indicated that a tornado touched down east-southeast of the city, in the Castle Mountain Estates subdivision. The city's water tank, which is partially buried in the ground at the top of a nearby ridge, and another building that housed a water filtration system, were almost completely destroyed. As a result of the damage, the city was under a boil order through 8 June 2012. The approximate path of the tornado was 3-km (2 mi) long and 0.27-km (300 yd) wide. Debris was scattered in a path up to 0.45-km (500 yd) wide. The official rating of this tornado is EF-1, and related damage is illustrated in Fig. 18.

Two additional post-storm assessments were completed, including the rural Hobson/Moccasin and Big Sandy areas. In a rural area 4.8 km (3 mi) west-southwest of Hobson, trees were uprooted and snapped off and a garage was destroyed. No additional damage was observed between this location and Hobson. In Hobson, several larger cottonwood trees were uprooted or snapped off and several homes were damaged owing to trees falling onto the structures. The assessment team concluded that the damage in these locations was more consistent with strong straight-line winds from a macroburst, with estimated wind gusts at

Figure 18. Image of tornado damage near White Sulphur Springs. Image courtesy of NWS Great Falls.

51 m s^{-1} (115 mph). Farther north, approximately 8 km east of Denton, a building was destroyed with debris blown across the highway; however, this debris was associated with straight-line winds as all debris was blown in the same direction (north-northeast of the structure), consistent with the storm motion at that time. An observed tornado southeast of this location was in an area with no structures (Fig. 19). This tornado had an estimated 5-km long path and 0.36-km (400 yd) width. No damage or debris path was noted and the tornado was rated EF0.

Figure 19. Damage (left photo) from straight-line winds in excess of 45 m s^{-1} (100 mph) and baseball-sized hail (center photo) occurred from a macroburst near Hobson and Utica. These two images are courtesy of NWS Great Falls. A storm chaser captured a photo of a tornado (right, courtesy of R. Hill) around 0012 UTC 6 June 2012 in northeastern Judith Basin County.

The final tornado that was assessed impacted locations in rural Chouteau County, approximately 26 km southeast of Big Sandy (Fig. 20), with reports of tree and home damage. These trees were snapped, twisted off, and uprooted with large branches tossed up to 0.36 km (400 yd) from their origin. The approximate tornado path was 1.6-km long and 0.07-km (75 yd) wide, with a debris path up to 0.09-km (100 yd) wide. This tornado was rated EF0, with damage shown in Fig. 21.

Figure 20. Photograph of tornado near Big Sandy from area storm chasers (courtesy of J. Risley).

The NWS in Great Falls received a photograph of this tornado with associated damage shown in Fig. 21. A rancher in the area, approximately 5 km east of Warrick in Chouteau County, reported that trees also were uprooted and snapped off at his ranch. The assessment team noted that the damage at the ranch was a result of the strong straight-line winds corresponding with a macroburst that continued to accompany the eastern side of the storm.

6. Impact-based decision support services

Forecast models began to indicate the potential for a widespread severe weather event for north-central Montana on 4 June 2012. NWS Great Falls performed several impact-based decision support services (IDSSs) leading up to the event to alert NWS partners and the general public of the potential threat. On 31 May 2012, NWS Great Falls issued an e-mail notification to partners (e.g., emergency managers and the media) that longer-range weather models were beginning to indicate a weather pattern that is favorable for strong to severe thunderstorms early the

Figure 21. Trees were snapped and uprooted in the Eagle Creek drainage 26 km (16 mi) southeast of Big Sandy. Images courtesy of NWS Great Falls.

following week. An update to this e-mail notification was sent on 3 June 2012 and continued to advertise the possibility for strong to severe thunderstorms across north-central Montana, with increasing confidence. In addition, a graphical depiction of impactful weather, known as a "Weather Story" (e.g., Fig. 22), was created on 3 June 2012—along with a recorded weather briefing that discussed the potential severe weather hazards for the entire state of Montana.

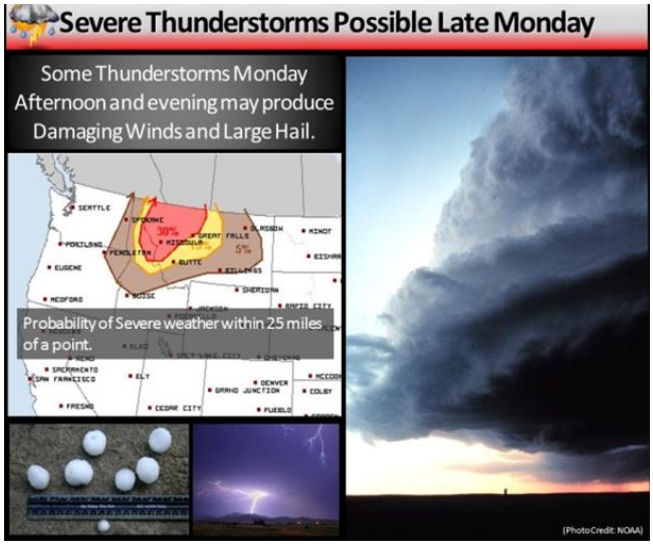

Figure 22. Weather Story created by NWS Great Falls on 3 June 2012 highlighting the potential severe weather threat for 5 June 2012.

While NWS Great Falls did not receive feedback regarding its IDSSs, this was the first major convective outbreak to affect central Montana since IDSS-related activities had spun up at this office. The statewide weekly weather briefing concept was very new for the Great Falls office, and this represented one of the office's first attempts at disseminating severe weather information using social media. This also was the first substantial tornado event that occurred in the Great Falls forecast area after NWS began using social media in 2011. Despite the paucity of feedback received, the population density is scarce in the areas affected by the tornadoes. For example, the population density for Chouteau County is 1 person per km^2, and for both Judith Basin and Meagher Counties it is <1 person per km^2. Given the rural nature of the areas affected and infancy of the IDSS program, it is not surprising that feedback was limited for this event.

7. Conclusions

The combination of a strong midlevel ridge over the northern plains, an enhanced surface lee trough over the northern Rockies, ample deep moisture, CAPE, and low-level wind shear over central Montana was associated with an environment favorable for organized, supercell thunderstorms that produced three tornadoes on 5 June 2012. It is rather rare for these ingredients to align in central Montana.

Daily mean values of various meteorological parameters—when compared to long-term means—indicated anomalously high 500-hPa heights accompanying a ridge downstream from central Montana, with very anomalously steep midlevel lapse rates over central Montana. Anomalously high PWAT values also were found to be associated with this environment, with relatively rich low-level moisture supporting sufficient buoyancy for severe thunderstorms amidst at least modest amounts of low-level and deep shear.

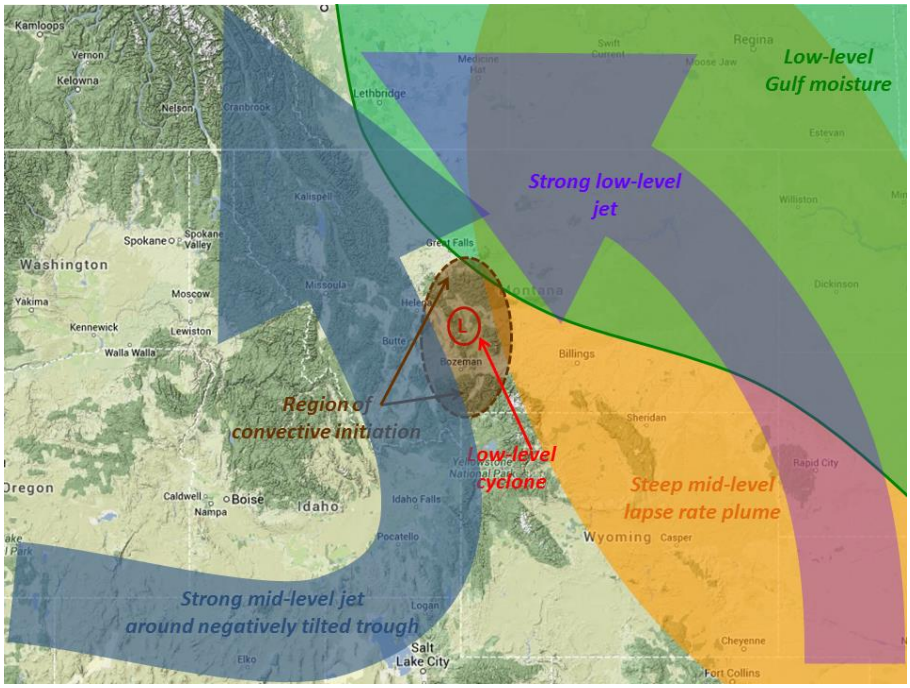

Figure 23. Schematic of salient features supporting the 5 June 2012 severe weather event around the time of convection initiation.

The favorable alignment of instability, moisture, lift, and vertical wind shear supported three tornadoes that occurred from two distinct long-track supercells tracking over rural areas of complex terrain. Radar analyses indicated that multiple strong gate-to-gate shear values occurred at various times through the long-duration mesocyclones accompanying tornadic supercell structures. From a historic perspective, the longevity and intensity of such structures is exceedingly rare in this part of the United States. This study highlights the nature of patterns that would support such an event, including their climatological context, with the hopes of anticipating any similar events in the future. As an attempt to synthesize all of these ingredients presented herein, Fig. 23 provides a schematic for forecasters that summarizes relevant concepts in anticipating these events.

Acknowledgments. Upper-air analyses were obtained from the SPC website (www.spc.noaa.gov/obswx/maps/). Tornado reports were plotted with SPC's SeverePlot 3.0 (www.spc.noaa.gov/climo/online/sp3/plot.php). The base map for the schematic shown in Fig. 23 originated from Google Maps (maps.google.com/). The authors thank (i) Dr. Israel Jirak of the SPC for his review and suggestions for improvement of this work and (ii) the staff at NWS Great Falls for research assistance and reviews of this paper.

REFERENCES

Banta, R. M., and C. B. Schaaf, 1987: Thunderstorm genesis zones in the Colorado Rocky Mountains as determined by traceback of geosynchronous satellite images. *Mon. Wea. Rev.*, **115**, 463–476.

Bosart, L. F., A. Seimon, K. D. LaPenta, and M. J. Dickinson, 2006: Supercell tornadogenesis over complex terrain: The Great Barrington, Massachusetts, tornado on 29 May 1995. *Wea. Forecasting*, **21**, 897–922.

Carbin, G. W., cited 2013: Storm Prediction Center WCM Page. [Available online at www.spc.noaa.gov/wcm/.]

Lemon, L. R., 1998: The radar "three-body scatter spike": An operational large-hail signature. *Wea. Forecasting*, **13**, 327–340.

Mesinger, F., and Coauthors, 2006: North American Regional Reanalysis. *Bull. Amer. Meteor. Soc.*, **87**, 343–360.

Thompson, R. L., R. Edwards, J. A. Hart, K. L. Elmore, and P. Markowski, 2003: Close proximity soundings within supercell environments obtained from the Rapid Update Cycle. *Wea. Forecasting*, **18**, 1243–1261.

Tucker, D. F., and N. A. Crook., 2001: Favored regions of convective initiation in the Rocky Mountains. Preprints, *9th Conf. on Mesoscale Processes*, Fort Lauderdale, FL, Amer. Meteor. Soc., 10.8. [Available online at ams.confex.com/ams/pdfpapers/22784.pdf.]